Multivariate processing of magnetotelluric data – comparison and interpretation of measurement results from the Westerwald (Germany)

Philip Hering[1], Andreas Junge[1], Nynne Lauritsen[2], Annika Löwer[1]

(1) Institute of Geosciences, Applied Geophysics, Goethe University Frankfurt am Main, Germany
(2) DTU Space, Technical University of Denmark, Denmark

Summary

During the processing of magnetotelluric (MT) data, frequency-dependent, complex transfer functions between magnetic (B) and electric (E) fields are calculated. The transfer functions provide information about the conductivity of the subsurface and thus are of crucial importance. In some cases the data processing proves to be difficult, since the recorded time series can be heavily contaminated by anthropogenic noise signals, e. g. galvanic currents or near field sources. Several methods, like robust or remote reference processing, address these problems, however in case of coherent noise sources they might fail (*Junge, 1996*). Therefore a new multivariate processing scheme based on an eigenvalue decomposition method (*Egbert, 1997*) was developed within an AMT study in the Westerwald, Germany (*Hering, 2015*). The results are presented for frequencies between 10 Hz and 5 kHz. The choice of the noise model is crucial for noise being coherent between different channels at a local site but incoherent to that at remote sites. For an unfavorable signal-to-noise ratio, however, the results of the eigenvalue analysis might be misleading, e. g. if the two dominant eigenvalues are taken as an indication for homogeneous source fields. Furthermore the magnetic and electric field polarizations from the Westerwald data set were analyzed. The results show distinct preferential directions and may be related to artificial source fields. As a consequence the far field assumption has to be checked for subsequent data interpretation.

Introduction

Principally the evaluation of magnetotelluric data is based on the calculation of transfer functions (TF) between electric and magnetic fields. For example the measured horizontal electric and magnetic field components (E_x and E_y, resp. B_x and B_y) are related by the frequency dependent impedance tensor ($\underline{Z}$) (e. g. *Tikhonov and Berdichevsy, 1966*):

$$\begin{pmatrix} E_x \\ E_y \end{pmatrix} = \begin{pmatrix} Z_{xx} & Z_{xy} \\ Z_{yx} & Z_{yy} \end{pmatrix} \begin{pmatrix} B_x \\ B_y \end{pmatrix} \quad (1)$$

All the variables are defined in frequency domain and the components $Z_{i,j}$ (i = x,y and j = x,y) of the impedance tensor represent the magnetotelluric transfer functions. The complex impedance values are visualized by the period (T) dependent phase- (φ) and apparent resistivity- (ρ_a) curves:

$$\varphi_{ij} = tan^{-1} \frac{\mathfrak{C}(\tilde{Z}_{ij})}{\Re(\tilde{Z}_{ij})} \quad (2)$$

$$\rho_{a,ij} = 0.2\, T\, |Z_{ij}|^2 \quad (3)$$

Generally $Z_{i,j}$ are estimated by a bivariate linear approach resulting from eq. (1), where the electric fields are assumed to contain noise while the magnetic fields are regarded as noise-free. Noise in the magnetic channels violates this assumption and causes the underestimation of the transfer functions (bias effects). One way to handle this problem is the remote reference method (e. g. *Gamble et al., 1979*). Subsequently robust methods can be applied to the processing scheme by predefined selection criterions choosing short time windows of the entire time series (e. g. *Junge, 1992*, *Ritter et al., 1998*, *Löwer, 2014*). A commonly used criterion is based on coherency between the electric and magnetic fields. Generally this method yields good results, but in case of coherent noise between the electric and magnetic field channels, it might fail. This also applies to the remote reference method mentioned before: if the noise is coherent between the local and the remote site (e.g. if the distance between the local and the remote site is too small), the method yields unsatisfying results.

In June/July 2014 magnetotelluric measurements were performed in the Westerwald, which is part of the Rhenish Massif in central Germany. The survey area was located at a geological fault zone with steeply dipping shales near the surface. The measurement campaign aimed at the detection of three-dimensional, anisotropic conductivity structures and the comparison with geoelectric measurements in the same area. As the experiment focused on the near-surface, mainly frequencies between 10 Hz and 5 kHz were investigated.
In **Fig. 1** transfer functions resulting from a standard robust processing scheme (*Löwer, 2014*) are shown for the off-diagonal tensor elements. Beside large scatter, the phases take very low values which is most commonly a clear indication for anthropogenic noise sources and nearfield effects. For further investigation of the nature of the noise sources, a multivariate processing scheme is presented in the next section (following *Egbert, 1997*).

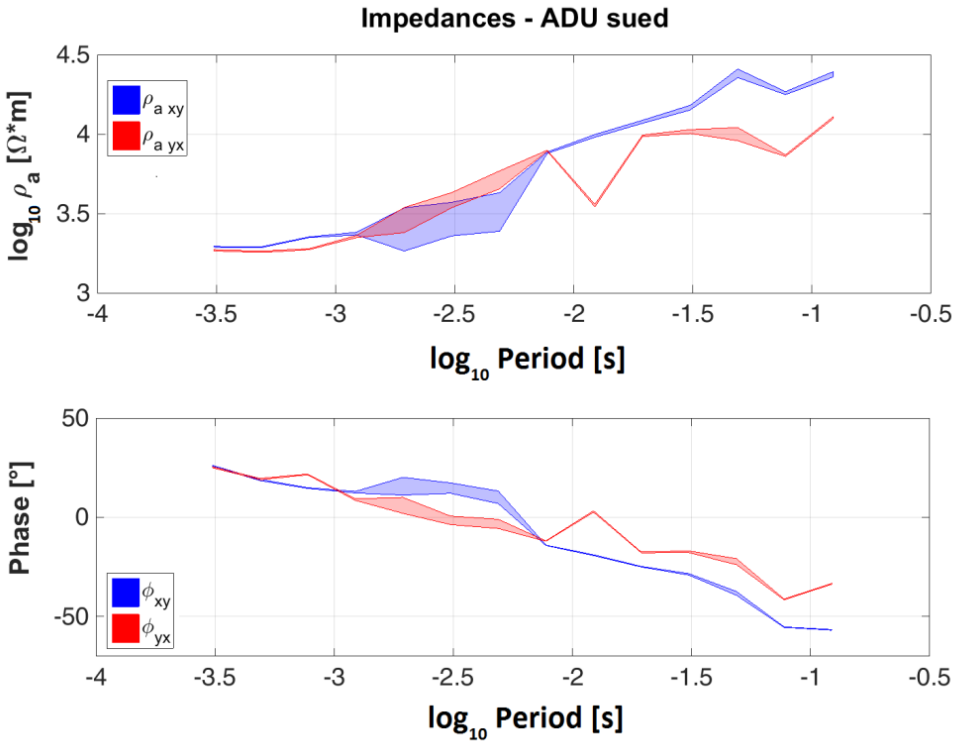

Fig. 1: Transfer functions for site "ADU sued" (Westerwald campaign 2014) as phase- and ρ_a-curves with 95%- confidence intervals (shaded areas) . The time series had been bandpass filtered (LP: 5 kHz, HP: 6 Hz) and the processing consisted of a robust bivariate calculation of the transfer functions based on a coherency selection criterion.

Multivariate processing

Following *Egbert* (*1997*) the multivariate processing scheme is based on the idea of using as many stations and channels (generally 3 magnetic and 2 electric channels for each station) as possible in view of detecting and removing incoherent noise from the data. The processing algorithm detects the number of independent polarizations within the source field by solving a generalized eigenvalue problem. With absent coherent noise and for a homogeneous source, not more than two dominant Eigenvalues significantly larger than 1 should occur (*Egbert, 1997*).
Equation (4) describes the idea behind the processing for a given data vector X_i of MT observations $e_{j,i}$ and $b_{j,i}$.

$$X_i = \begin{pmatrix} e_{1,i} \\ b_{1,i} \\ \vdots \\ e_{J,i} \\ b_{J,i} \end{pmatrix} = \begin{pmatrix} \xi_{1,1} \\ \eta_{1,1} \\ \vdots \\ \xi_{J,1} \\ \eta_{J,1} \end{pmatrix} * \beta_{1,i} + \begin{pmatrix} \xi_{1,2} \\ \eta_{1,2} \\ \vdots \\ \xi_{J,2} \\ \eta_{J,2} \end{pmatrix} * \beta_{2,i} + \varepsilon_i = U\beta_i + \varepsilon_i \qquad (4)$$

With *J* as the number of stations *j*, *i*: index of the time segment, e and b the Fourier coefficients of the electric and magnetic fields, β describing the two polarizations of the natural MT-source fields, ε as the residual, containing all noise parts.

Equation (5) allows for coherent noise being attributed to the signal, as in practice both cannot be distinguished easily. The residual ε is reduced to the incoherent noise part.

$$X_i = \mathrm{U}\beta_i + \mathrm{V}\gamma_i + \varepsilon_i = [U \quad V]\begin{bmatrix}\beta_i \\ \gamma_i\end{bmatrix} + \varepsilon_i = \mathrm{W}\alpha_i + \varepsilon_i \tag{5}$$

Now *U* contains the natural signal and *V* contains the coherent noise, γ_i represents the polarizations of the noise source fields whereas α_i is the vector combining natural and noise source field polarizations

Before starting the eigenvalue analysis, all time series are bandpass filtered. Then the whole processing is performed in the frequency domain evaluating each target frequency separately. Initially the spectral density matrix (*S*) is calulated containing all the cross- and auto spectra from all the channels:

$$S = \begin{bmatrix} b_{x1,i} * b^*_{x1,i} & b_{y1,i} * b^*_{x1,i} & \cdots & e_{xK,i} * b^*_{x1,i} & e_{yK,i} * b^*_{x1,i} \\ b_{x1,i} * b^*_{y1,i} & b_{y1,i} * b^*_{y1,i} & & e_{xK,i} * b^*_{y1,i} & e_{yK,i} * b^*_{y1,i} \\ \vdots & & \ddots & \vdots & \\ b_{x1,i} * e^*_{xK,i} & b_{y1,i} * e^*_{xK,i} & & e_{xK,i} * e^*_{xK,i} & e_{yK,i} * e^*_{xK,i} \\ b_{x1,i} * e^*_{yK,i} & b_{y1,i} * e^*_{yK,i} & \cdots & e_{xK,i} * e^*_{yK,i} & e_{yK,i} * e^*_{yK,i} \end{bmatrix} \tag{6}$$

With *e, b* the electric and magnetic field Fourier coefficients, *K* the number of channels (generally 5**J*)

The spectral density matrix is normalized by the noise covariance matrix ΣN (see next chapter) and the eigenvalue problem (7) can be formulated:

$$S * u = \lambda * \Sigma_N * u \tag{7}$$

Here λ contains all the eigenvalues which can be interpreted as a signal to incoherent noise ratio and *u* stands for the corresponding eigenvectors. In case that only two dominant eigenvalues exist, the rescaled data vector *U (*see (4)) is derived from the two corresponding eigenvectors represented by *U'*.

$$U = \Sigma_n^{1/2} * U' * (U' * \Sigma_n^{-1} * U')^{-1} \tag{8}$$

In the last step, transfer functions *Z* for each site *J* are calculated from *U* accounting for the particular electric and magnetic fields:

$$Z_J = \begin{bmatrix}\xi_{xJ1} & \xi_{xJ2} \\ \xi_{yJ1} & \xi_{yJ2}\end{bmatrix} * \begin{bmatrix}\eta_{xJ1} & \eta_{xJ2} \\ \eta_{yJ1} & \eta_{yJ2}\end{bmatrix}^{-1} \tag{9}$$

Two different models for incoherent noise estimation

The estimation of the noise covariance matrix is of essential importance for the calculation of reliable transfer functions. In the following we present two models for to assess the incoherent noise level for each of the observed field components.

In a first approach we assume incoherent noise between all the existing field components. The noise covariance matrix (ΣN) is calculated by a multiple linear regression for each component (*k*) against the remaining (*K-1*) components. The variances of the residuals are summarized by:

$$\Sigma_N = \begin{bmatrix} \sigma_1^2 & 0 & \cdots & 0 & 0 \\ 0 & \sigma_2^2 & & 0 & 0 \\ \vdots & & \ddots & \vdots & \\ 0 & 0 & & \sigma_{K-1}^2 & 0 \\ 0 & 0 & \cdots & 0 & \sigma_K^2 \end{bmatrix} \quad (10)$$

With: $\sigma_1^2 \ldots \sigma_k^2$ as the noise variances for each component.

Allowing for coherent noise between the field components at each station, the multiple linear regression is modified such that each of the 5 components of the station is predicted by the (K-5) components of the remaining sites. The modified analysis yields the covariance matrix for each site which can be summarized by the block diagonal matrix:

$$\Sigma_N = \begin{bmatrix} \sigma_1^2 & \sigma_{1,2}^2 & \sigma_{1,3}^2 & & & 0 & 0 & 0 \\ \sigma_{2,1}^2 & \sigma_2^2 & \sigma_{2,3}^2 & \cdots & & 0 & 0 & 0 \\ \sigma_{3,1}^2 & \sigma_{3,2}^2 & \sigma_3^2 & & & 0 & 0 & 0 \\ & \vdots & & \ddots & & \vdots & & \\ 0 & 0 & 0 & & \sigma_{K-2}^2 & \sigma_{K-2,K-1}^2 & \sigma_{K-2,K}^2 & \\ 0 & 0 & 0 & \cdots & \sigma_{K-1,K-2}^2 & \sigma_{K-1}^2 & \sigma_{K-1,K}^2 & \\ 0 & 0 & 0 & & \sigma_{K,K-2}^2 & \sigma_{K,K-1}^2 & \sigma_K^2 & \end{bmatrix} \quad (11)$$

With each components' variances of the residuals on the main diagonal and the covariances on the off diagonals.

The application of covariance model (11) proved to be crucial for the transfer function estimation of some of our data sets.

Results

The multivariate processing scheme was applied to data sets from the MT survey in the Westerwald in 2014. They were obtained at two stations ("ADU sued" and "ADU west") which were approximately 350 m apart. At both sites 3 magnetic (H_x, H_y, H_z) and two electric field (E_x, E_y) components were recorded with a sampling rate of 16 kHz. The length of the time series was 15 minutes with noise occurring permanently during the observation period. Therefore the division into individual subintervals was omitted. Before the multivariate processing the data was bandpass filtered (LP: 6 kHz, HP: 10 Hz).

The Eigenvalues resulting from two different noise models are compared and presented in Fig. 2. Noise model 1 refers to the simple case (cf. equation (10)) and yields more than 2 dominant eigenvalues for the whole frequency range (Fig. 2(a)). We assume that the data is strongly influenced by coherent noise signals. The calculation of the data vector *U* (eq. (8)), using the two largest eigenvectors results in impedances which are highly contaminated, especially the phase curves (**Fig. 3**). Using the noise covariance matrix of model 2 (cf. equation (11)) produces two dominant eigenvalues clearly separated from the remaining eigenvalues (Fig. 2(b)). Therefore we assume that they represent the polarizations of the source field. Noise model 2 improves the impedances significantly (**Fig. 4**), also with respect to the standard robust processing procedure (**Fig. 1**). Nevertheless, the phase curves still decay steeply towards zero with decreasing frequency, which can be an indication for nearfield effects. Furthermore the polarization directions of the electric (E) and magnetic (B) fields were analyzed. They were calculated for each Fourier coefficient according to *Fowler (1967*) (eq. (12), shown for the electric field):

$$\Psi = \tan^{-1}\left(\frac{2*\Re(E_x*E_y^*)}{|E_x|^2-|E_y|^2}\right) \qquad (12)$$

They have distinct preferential directions as well for the electric as for the magnetic field (Fig.5). As for natural source fields the polarization directions of the magnetic field are assumed to be randomly distributed, we suspect that the transfer functions related to the two dominant eigenvalues result from artificial source fields. This would implicate that the two dominant eigenvalues do not necessarily indicate homogeneity of the source field. The origin of the artificial signals is uncertain. They could be led back to the disadvantageous signal-to-noise ratio due to the AMT-dead-band between 1 kHz and 5 kHz. Another explanation could be an electric current channeling effect due to the steeply inclined shales at the near surface. This assumption could be an interesting target for a theoretical study.

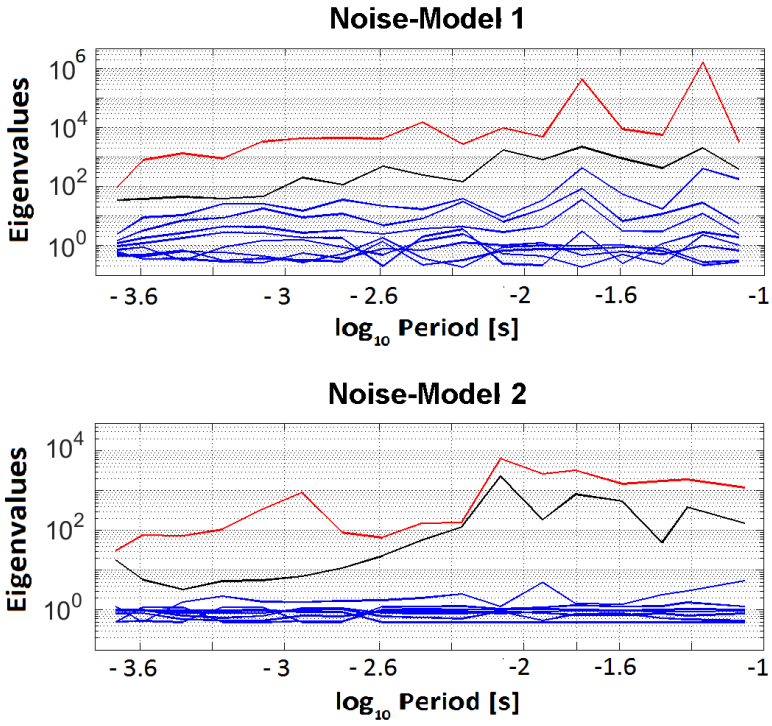

Fig. 2: Eigenvalue analysis using two different Noise-Models. Dominant eigenvalues 1 and 2 are marked in red and black. The calculation is based on data observed at stations "ADU sued" and "ADU west" from the measurement campaign in the Westerwald (2014). **Top (a)**: Only incoherent parts of the noise. **Bottom (b)**: Coherent noise allowed within one station.

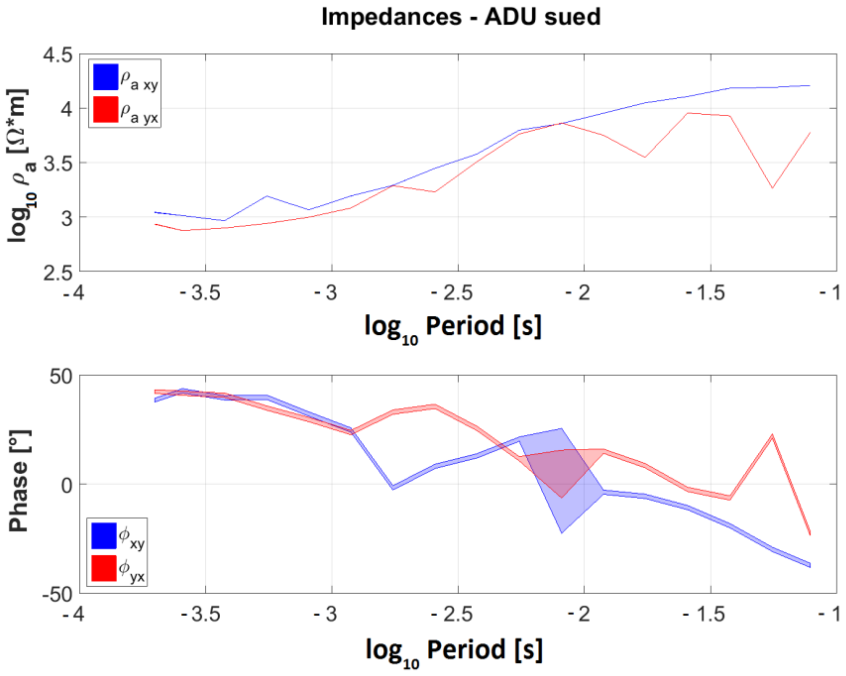

Fig. 3: Transfer functions for site "ADU sued", shown in form of phase- and ρ_a- curves from **Noise-Model 1**. The shaded areas represent the 95%- confidence intervals. The multivariate processing was performed using the stations "ADU sued" and "ADU west" from the 2014-measurement campaign in the Westerwald.

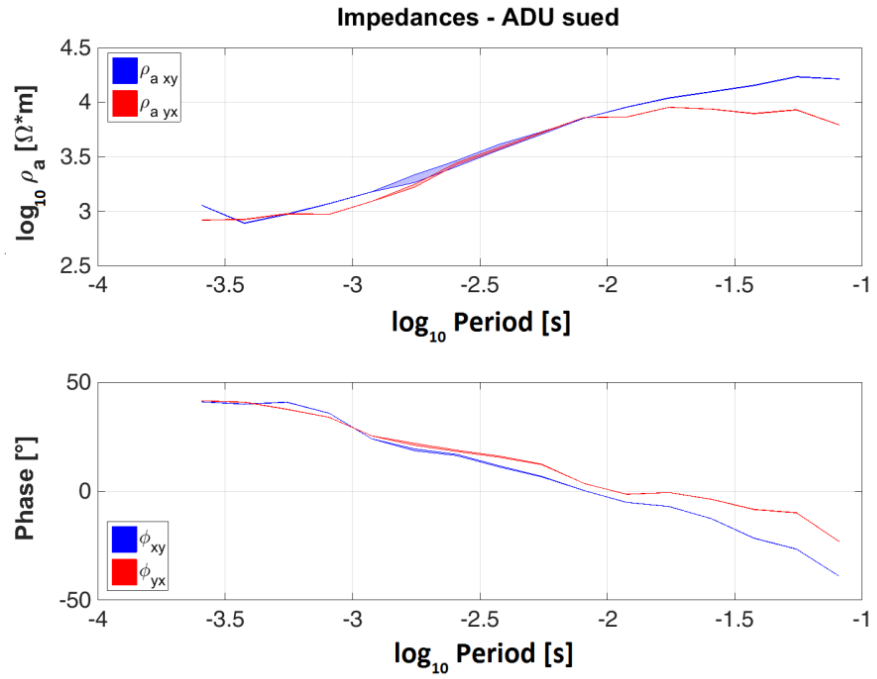

Fig. 4: Transfer functions for site “ADU sued” as in Fig.3 using **Noise-Model 2**.

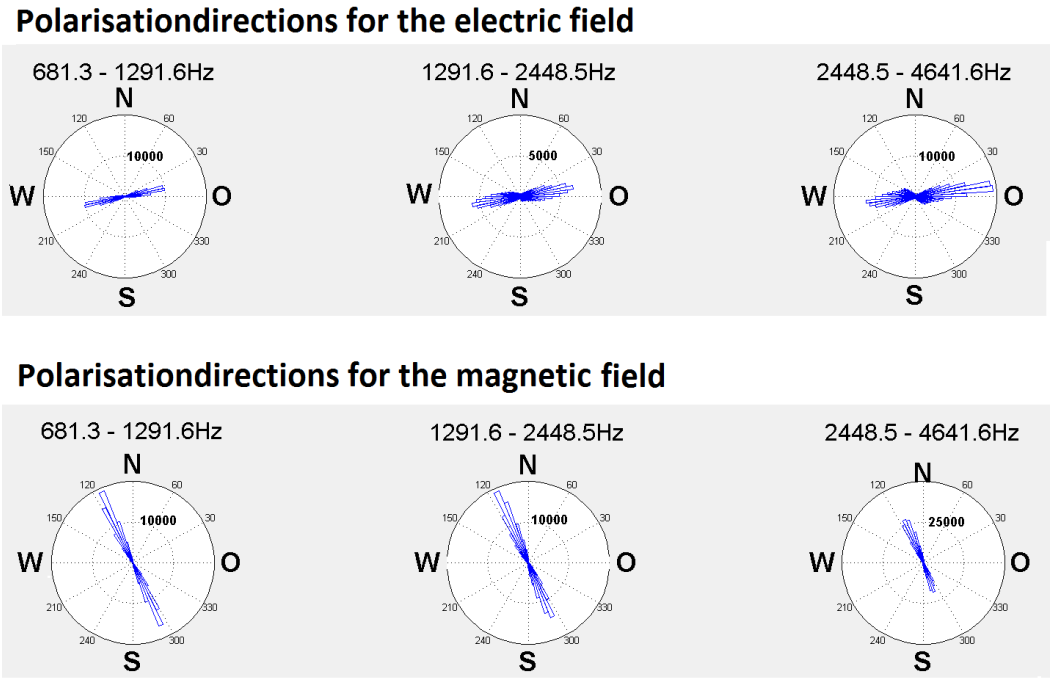

Fig 5: Polarizations of the electric (**top**) and magnetic fields (**bottom**) from station “ADU sued” are showing strongly preferred directions. The polarization direction of the fields was calculated for each Fourier coefficient. The results are summarized in three rose plots with frequency ranges above 680 Hz and a cluster width of 4°.

Conclusions

The presented multivariate processing scheme removes incoherent noise from the data and indicates the presence of coherent noise sources. The example from the Westerwald shows a significant improvement for the transfer function estimation compared to the standard robust single site processing. Here the choice of the noise model is of crucial importance. Using a noise covariance matrix which considers coherent noise signals between the field-components observed at one station is strongly recommended. However, two distinct dominant eigenvalues might also represent a high anthropogenic noise level in case of very weak natural signals. It is recommended to check the polarization directions of the magnetic fields for distinct preferred directions which might indicate strong influence from anthropogenic noise. In case of the data set from the Westerwald, the recorded signals were mostly referred to artificial source fields. As a consequence the interpretation of the data was restricted to frequencies above 1 kHz to fulfill the far field assumption.

Literature

Egbert, G. (1997), *Robust multiple-station magnetotelluric data processing*, Geophys. J. Int. 130, 475-496

Fowler, R., Kotick, B. and Elliot, R. (1967), *Polarization analysis of natural and artificially induced geomagnetic micropulsations*, J. geophys. Res. 72

Gamble, T., Goubau, W. und Clarke, J. (1979), *Magnetotellurics with a remote reference*, Geophysics 44**,** 53-68.

Hering, Ph. (2015), *Magnetotellurische Messungen im Westerwald - Eine Studie zur Detektion und Minimierung von anthropogenen Rauschsignalen*, Master-Thesis (in German), Goethe University Frankfurt am Main

Junge, A. (1992), *Erweiterte Auswerteverfahren in Göttingen*, Tagungsband, 14. Kolloquium Elektromagnetische Tiefenforschung in Borkheide, Deutsche Geophysikalische Gesellschaft, ISSN: 0946 7467

Junge, A. (1996), *Characterization of and correction for cultural noise*, Surv. Geophys. 17, 361–391

Löwer, A. (2014), *Magnetotellurische Erkundung geologischer Großstrukturen des südwestlichen Vogelsberges mit anisotroper, dreidimensionaler Modellierung der Leitfähigkeitsstrukturen*, PhD-Thesis (in German), Goethe University Frankfurt am Main

Ritter, O., Junge, A. and Dawes, G. J. (1998), *New equipment and processing for magnetotelluric remote reference observations*, Geophys. J. Int. 132**,** 535-548

Tikhonov, A. N. und Berdichevsky, M. (1966), *Experience in the use of magnetotelluric methods to study the geological structures of sedimentary basins*, Izv. Acad. Sci. USSR, Phys. Solid Earth 2**,** 34-41